Scientific Journals
of the Maritime University of Szczecin

Zeszyty Naukowe
Akademii Morskiej w Szczecinie

2016, 46 (118), 9–16
ISSN 1733-8670 (Printed)
ISSN 2392-0378 (Online)
DOI: 10.17402/111

Received: 31.08.2015
Accepted: 10.03.2016
Published: 27.06.2016

The linearization of mooring load distribution problem

Jarosław Artyszuk

Maritime University of Szczecin
1–2 Wały Chrobrego St., 70-500 Szczecin, Poland, e-mail: j.artyszuk@am.szczecin.pl

Key words: ship manoeuvring, mooring, berthing, hydrodynamics, loads, linear model, linearization

Abstract

This paper presents a novel step forward in finding the loads of particular mooring ropes that balance the steady environmental excitations for a ship staying at berth. The industrial static equilibrium method for a rough assessment of ship mooring safety is considered to be well-established. The static loads are directly related to the rope's MBLs (minimum breaking loads) while applying a certain safety margin (usually 50%). The problem is reduced to a set of linear equations that may be solved analytically. The generality in terms of arbitrary horizontal and vertical angles of mooring ropes is preserved. All derivations are provided to enhance trust in the very simple yet absolutely accurate and fast linear solution. The accuracy is studied both analytically, throughout all the development stages, and finally by comparison to the exact numerical solution of the original nonlinear equilibrium equations for an exemplary mooring pattern. A discussion of selected effects in load distribution is also given. Using the approach presented, for instance, we can efficiently test mooring safety when any mooring rope of the set is accidentally broken.

Introduction

The ship navigators and berth/terminal operators are often faced with the problem of excessive loads in mooring ropes in both common and extreme weather conditions. Guidance is needed, for both the design of new technical systems and the operation of a currently existing situation. In both cases, various risk/failure options must be considered. One method of practical importance is the static equilibrium analysis of a moored ship. The geometry of mooring lines with no catenary effect (i.e. the straight line) is generally assumed here for merchant ships.

The ship's static equilibrium can be examined by means of ship manoeuvring simulation, e.g. (Artyszuk, 2004), or through purely static methods (Chernjawski, 1980; OCIMF, 2013). In both cases, we only and directly determine a ship's linear and angular offset from a berth, which results in stretching mooring ropes so as to balance the environmental load. The subsequent computation of particular rope tensions is straightforward.

In the both the mentioned approaches the use of time-consuming numerical methods is required. In the first case, they deal with a set of ordinary differential equations in time-domain; in the second one, a set of algebraic equations is solved.

Although the adopted formulation of the mooring problem is not explicitly called linear in the studies of (Chernjawski, 1980), and in those reproduced by (Natarajan & Ganapathy, 1995), the matrix equations used (which inherently present some linearizations) and the simple input data uniquely lead to a fully linear problem that can be solved analytically. However, for reasons that are not explained, a numerically iterative (or incremental) technique is undertaken, in threference cited works, to solve the problem.

The analytical methods for linear problems are very fast and exact, allowing for various efficient parametric studies. If possible, they should be always encouraged. Moreover, they are readily available for everyone, even for an inexperienced user. On the other hand, the consequences and validity range of the linearizations made to the mooring problem,

which should be thoroughly understood, have not been fully appraised so far in literature.

That is why in the present paper a careful, systematic development (through successive approximations) of the linear mooring model is challenged, starting from a nonlinear model. The evaluation is made analytically (while discussing the simplifications) and numerically, for a specific case study.

Mooring force model for a ship's arbitrary movement

In order to develop a full nonlinear model of the mooring rope effect on a ship, we introduce two 2D reference systems – *Mxy* and *OXY*, see Figures 1 and 2. Both are placed in the horizontal, top-view plane of water. The former is ship-fixed and used for defining locations of the ship's fairleads and for expressing the exciting forces acting on it. The latter coordinate system is earth-fixed and used for motion description, but only in terms of the ship's position and attitude geometric variations. By default, the *OXY* system is the primary one used for performing the below vector calculations. The use of the local system *Mxy* (whenever necessary) will be explicitly marked in the formulas. It is assumed that *Mxy* and *OXY* initially coincide and are aligned with each other, i.e. *OXY* is naturally positioned at the ship's origin while the ship is alongside the berth in calm weather. In this case, the ship is slightly touching the

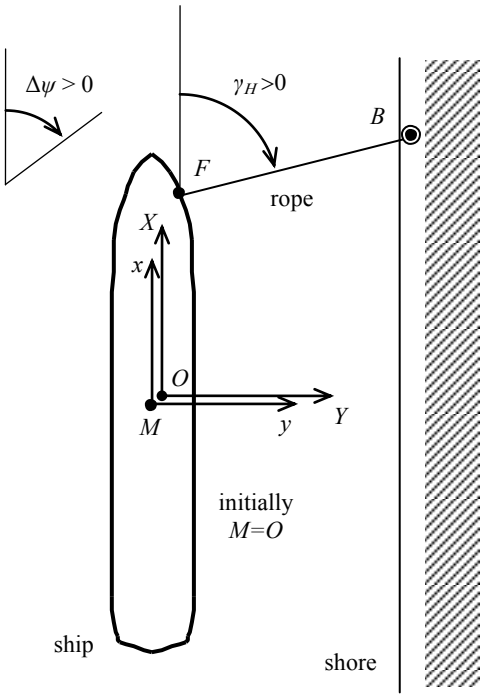

Figure 1. Reference systems and basic definitions

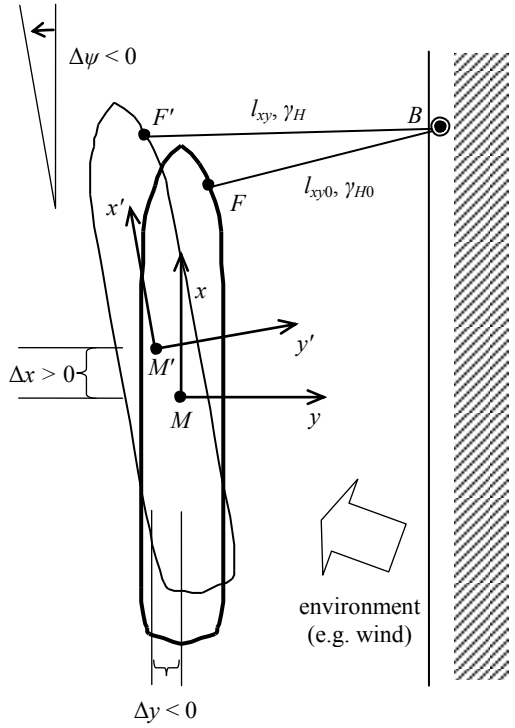

Figure 2. Geometry of ship's departure from origin – general case

fenders and has marginal tension in mooring ropes. The *X*-axis corresponds to the direction of the berth line. The angular displacement of the ship to starboard ($\Delta\psi$) and the horizontal angle of the rope (γ_H) if made fast on starboard side are both given a positive value.

The mentioned nonlinearity of the model derives from the geometric relations involved in the system consisting of the ship's fairlead (*F*), shore-based bollard (*B*), and mooring rope connecting the two. The nonlinearity is especially evident in the case of a fairly large movement of the ship away from the berth – Figure 2. In mechanical aspects, however, the linear law of rope elasticity (strain-stress characteristics) is usually adopted, and also used hereafter.

In Figure 2, an example of the new linear and angular positions of the ship is denoted by the prime-sign ('). Determination of the possible causes of such extreme and sudden departure from the original situation ($M = O$, $Mx \parallel OX$) is beyond the scope of the present work. Although the ship starts to drift due to wind, and its track initially follows roughly the direction of the wind (with some heading alteration based on wind moment), the mooring rope immediately begins stretching and restrains further movement of the ship. The improper, hypothetical scale of the ship's movement, depicted in Figure 2, is uncommon in mooring practice but is nevertheless convenient for defining appropriate relationships

within the model and is intended to constitute a firm background for reasonable linearization. In particular, Figure 2 shows variations of the horizontal angle (see Figure 1), depicted as γ_H (actual) and γ_{H0} (initial), and in the horizontal plane projection of the 3D rope, represented by its projection lengths – l_{xy} and l_{xy0}. The figure also shows the linear (Δx, Δy) and angular displacements of the ship in this situation, to facilitate the interpretation of the provided numerical results.

The evolution of the fairlead coordinates on earth can be written using the following vectorial notation (see Figure 3):

$$\mathbf{r_F} = \mathbf{r_M} + \mathbf{r_{MF}} \tag{1}$$

$$\mathbf{r_F} = \begin{bmatrix} x_{Fo} \\ y_{Fo} \end{bmatrix}, \quad \mathbf{r_M} = \begin{bmatrix} \Delta x \\ \Delta y \end{bmatrix},$$
$$\mathbf{r_{MF}} = \begin{bmatrix} \cos\Delta\psi & -\sin\Delta\psi \\ \sin\Delta\psi & \cos\Delta\psi \end{bmatrix} \cdot \begin{bmatrix} x_F \\ y_F \end{bmatrix}_{Mxy} \tag{2}$$

where $\mathbf{r_M}$, $\mathbf{r_{MF}}$, $\mathbf{r_F}$ stand for the vectors of the ship's origin shift; fairlead location versus ship's origin (with fixed coordinates of the fairlead in Mxy – x_F, y_F); fairlead location in OXY after the applied deviation in ship's position and heading, respectively.

The relative change of fairlead location, required for rope elongation calculations, reads:

$$\mathbf{\Delta r_F} = \mathbf{r_F} - \mathbf{r_{F0}} \tag{3}$$

where

$$\mathbf{r_{F0}} = \mathbf{r_F}(\Delta x = 0, \Delta y = 0, \Delta\psi = 0) = \\ = \begin{bmatrix} 1 & 0 \\ 0 & 1 \end{bmatrix} \begin{bmatrix} x_F \\ y_F \end{bmatrix} = \begin{bmatrix} x_F \\ y_F \end{bmatrix} \tag{4}$$

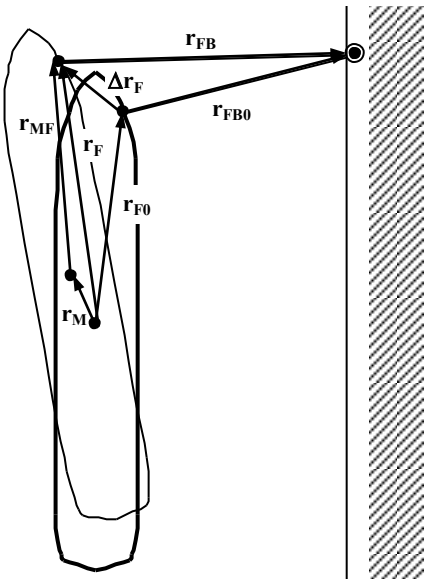

Figure 3. Vector analysis

Hence

$$\mathbf{\Delta r_F} = \begin{bmatrix} \Delta x \\ \Delta y \end{bmatrix} + \begin{bmatrix} \cos\Delta\psi & -\sin\Delta\psi \\ \sin\Delta\psi & \cos\Delta\psi \end{bmatrix} \cdot \begin{bmatrix} x_F \\ y_F \end{bmatrix} - \begin{bmatrix} x_F \\ y_F \end{bmatrix} \tag{5}$$

or

$$\mathbf{\Delta r_F} = \begin{bmatrix} \Delta x \\ \Delta y \end{bmatrix} + \begin{bmatrix} \cos\Delta\psi - 1 & -\sin\Delta\psi \\ \sin\Delta\psi & \cos\Delta\psi - 1 \end{bmatrix} \cdot \begin{bmatrix} x_F \\ y_F \end{bmatrix} \tag{6}$$

The vector $\mathbf{r_{FB}}$, symbolising the rope's orthogonal projection (of the fairlead-bollard 3D line) to the horizontal plane, is expressed by

$$\mathbf{r_{FB}} = l_{xy} \begin{bmatrix} \cos\gamma_H \\ \sin\gamma_H \end{bmatrix} = l\cos\gamma_V \begin{bmatrix} \cos\gamma_H \\ \sin\gamma_H \end{bmatrix}, \; l_{xy} = |\mathbf{r_{FB}}| \tag{7}$$

where the actual length, l_{xy}, serves as the basic intermediate unknown in our study of the ship's horizontal motion. Moreover, the initial horizontal estimate of l_{xy0} is usually given on input – i.e. based on the combined ship-terminal top view. The explicit knowledge of shore bollard coordinates is not needed at all. Note: the horizontal angle γ_H is counted against the earth-fixed axis OX.

As shown in Figure 4, this length can easily be turned into the total (3D) length l, necessary in further evaluations of the rope's elastic behaviour. Here, the key input is the fairlead-bollard vertical distance (height), Δh, which is always directly given. The bollards ashore, as well as the berth itself, are located much further below the ship's fairleads. Nevertheless, instead of the square root, it is often beneficial to introduce a proportionality coefficient between both lengths l_{xy} and l, and the resulting corresponding forces. This coefficient is the cosine of the vertical angle γ_V. The vertical angle changes in parallel with the total length while the ship undergoes a horizontal movement. Both l and γ_V are also included in (7).

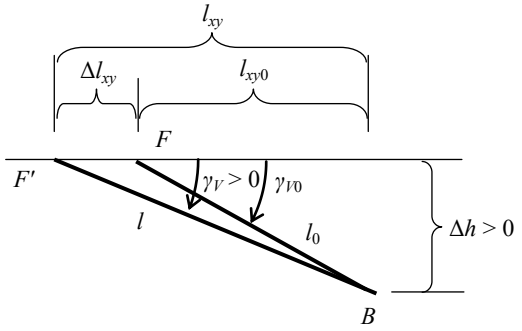

Figure 4. Situation in vertical plane of the rope

Similarly to Figure 2 and the related comments reported earlier, Figure 4 also illustrates a larger scale

of the ship's movement than the one seen during typical mooring.

The initial state of $\mathbf{r_{FB}}$ is marked by the use of the '0' sub-index in (7):

$$\mathbf{r_{FB}}_0 = l_{xy0}\begin{bmatrix}\cos\gamma_{H0}\\ \sin\gamma_{H0}\end{bmatrix} = l_0\cos\gamma_{V0}\begin{bmatrix}\cos\gamma_{H0}\\ \sin\gamma_{H0}\end{bmatrix},$$
$$l_{xy0} = \left|\mathbf{r_{FB0}}\right| \tag{8}$$

Finally

$$\mathbf{r_{FB}} = \mathbf{r_{FB0}} - \mathbf{\Delta r_F} \tag{9}$$

where the sign '–' at $\Delta\mathbf{r_F}$ arises from the fact that we 'move' the fairlead (not the bollard), as seen in Figure 4.

Introducing the increase in horizontal and total length:

$$\Delta l_{xy} = l_{xy} - l_{xy0},\ \Delta l = l - l_0 \tag{10}$$

and taking advantage of:

$$(\Delta h)^2 = l_0^2 - l_{xy0}^2 = l^2 - l_{xy}^2 \tag{11}$$

we can write:

$$l = \sqrt{(\Delta h)^2 + (l_{xy0} + \Delta l_{xy})^2} \tag{12}$$

$$\cos\gamma_V = \frac{l_{xy0} + \Delta l_{xy}}{\sqrt{(\Delta h)^2 + (l_{xy0} + \Delta l_{xy})^2}} \tag{13}$$

The relative elongation of the rope (responsible for developing the stress response) is thus:

$$\Delta l' = \frac{\Delta l}{l_0} = \frac{l}{l_0} - 1 \tag{14}$$

$$\Delta l' = \sqrt{\frac{l_0^2 - l_{xy0}^2 + (l_{xy0} + \Delta l_{xy})^2}{l_0^2}} - 1 \tag{15}$$

The expression of the rope load (and the force acting on the ship), according to the assumed linear elasticity, reads:

$$F = \Delta l' \cdot \frac{\mathrm{MBL}}{e_{\%}} \tag{16}$$

and its most interesting horizontal component (the mooring restraint force) takes the form:

$$F_{xy} = F\cdot\cos\gamma_V = \Delta l'\cdot\cos\gamma_V \cdot \frac{\mathrm{MBL}}{e_{\%}} \tag{17}$$

where MBL and $e_{\%}$ are the basic rope parameters – minimum breaking load (strength) and dimensionless specific elasticity, respectively. By definition, for $e_{\%} = 0.01\div0.02$ (typical for wire), we experience 1÷2% elongation of rope at MBL.

As can be seen in (17) on the right-hand side, the horizontal force is proportional to the product of two unknown terms, which can be rewritten as follows:

$$\Delta l' = \sqrt{1 + 2\frac{l_{xy0}}{l_0^2}\cdot\Delta l_{xy} + \frac{1}{l_0^2}\cdot(\Delta l_{xy})^2} - 1 \tag{18}$$

$$\cos\gamma_V = \frac{l_{xy0} + \Delta l_{xy}}{\sqrt{l_0^2 - l_{xy0}^2 + (l_{xy0} + \Delta l_{xy})^2}} = \frac{l_{xy0} + \Delta l_{xy}}{l_0\sqrt{1 + 2\frac{l_{xy0}}{l_0^2}\cdot\Delta l_{xy} + \frac{1}{l_0^2}\cdot(\Delta l_{xy})^2}} \tag{19}$$

from which we obtain a simple function of the variable Δl_{xy}:

$$\Delta l'\cdot\cos\gamma_V = \frac{l_{xy0} + \Delta l_{xy}}{l_0}\left(1 - \frac{1}{\sqrt{1 + 2\frac{l_{xy0}}{l_0^2}\cdot\Delta l_{xy} + \frac{1}{l_0^2}\cdot(\Delta l_{xy})^2}}\right) \tag{20}$$

Δl_{xy} is governed by l_{xy}, see (10) and (7), but according to (9), one gets:

$$\mathbf{r_{FB}} = \begin{bmatrix}X_{FB}\\ Y_{FB}\end{bmatrix} = \begin{bmatrix}l_{xy0}\cos\gamma_{H0} - \Delta x - (\cos\Delta\psi - 1)x_F + \sin\Delta\psi\cdot y_F\\ l_{xy0}\sin\gamma_{H0} - \Delta y - \sin\Delta\psi\cdot x_F - (\cos\Delta\psi - 1)y_F\end{bmatrix} \tag{21}$$

$$l_{xy} = \sqrt{X_{FB}^2 + Y_{FB}^2} \tag{22}$$

We do not intend here to settle the final expression for (22). The 'geometrically' derived non-linear, yet full, model of the single rope-excited mooring force F_{xy}, (17, 20–22, 10), explicitly provides the force value for a given ship position and heading change, as a function of three parameters (displacements) – Δx, Δy, $\Delta\psi$. This force, through the horizontal angle and application point (i.e. the fairlead), contributes to longitudinal, transverse, and rotational restraints of the ship in windy conditions. Although impractical, the static equilibrium in case of a single rope is theoretically possible and solvable. The inverse problem consists here in computing the ship's three displacement components based on the provided environmental (external) force, which consists of two force and one moment components. In the case

of our nonlinear model of multiple ropes, this can only be accomplished numerically. However, the presence of a unique solution may not be guaranteed. Finally, the desired mooring load is a direct outcome of the resolved displacements.

Approximations towards linearization

The approximations introduced from here on mostly consist of applying values of some functional sequence limits to the equations in the preceding chapter. To simplify notation, we deliberately use '=' instead of '≈', unless required for clarity and consistency, especially for expressions within the same line.

Step 1

For a general angle α approaching zero, we can state that:

$$\cos\alpha - 1 \approx 0 \quad \text{while} \quad \sin\alpha \approx \alpha \tag{23}$$

One can numerically estimate, that at least within the range of 1° for the angle, the left-hand side of the first expression in (23) leads to values roughly 10^3 times lower than the second expression, so it may be disregarded. More accurately:

$$1 - \cos\alpha \approx \frac{\alpha^2}{2} \tag{24}$$

which can be proved by L'Hopital's rule and even found in some elementary textbooks, e.g. (Bronsztejn & Siemiendiajev, 1996). Expression (24) is an infinitesimal of higher order (exactly second) to the second expression in (23).

Incorporating (23) to (21, 22), we gain:

$$\mathbf{r_{FB}} = \begin{bmatrix} X_{FB} \\ Y_{FB} \end{bmatrix} = \begin{bmatrix} l_{xy0}\cos\gamma_{H0} - \Delta x + \Delta\psi \cdot y_F \\ l_{xy0}\sin\gamma_{H0} - \Delta y - \Delta\psi \cdot x_F \end{bmatrix} \tag{25}$$

$$l_{xy} = \sqrt{l_{xy0}^2 + \underline{\left(\Delta x - \Delta\psi \cdot y_F\right)^2} - 2\cos\gamma_{H0}\left(\Delta x - \Delta\psi \cdot y_F\right) + \underline{\left(\Delta y + \Delta\psi \cdot x_F\right)^2} - 2\sin\gamma_{H0}\left(\Delta y + \Delta\psi \cdot x_F\right)} \tag{26}$$

Step 2

Let us now remove in (26) the underlined infinitesimal quantities of higher/second order to the linear combinations of ship's displacements (in brackets). Hence, after some minor rearrangements, one gets:

$$l_{xy} = \sqrt{l_{xy0}^2 - 2\cos\gamma_{H0} \cdot \Delta x - 2\sin\gamma_{H0} \cdot \Delta y + -2\left(-\cos\gamma_{H0} \cdot y_F + \sin\gamma_{H0} \cdot x_F\right)\Delta\psi} \tag{27}$$

and following (10):

$$\Delta l_{xy} = l_{xy0}\left(\sqrt{1 - 2\frac{\cos\gamma_{H0}}{l_{xy0}} \cdot \Delta x - 2\frac{\sin\gamma_{H0}}{l_{xy0}} \cdot \Delta y + -2\frac{\left(-\cos\gamma_{H0} \cdot y_F + \sin\gamma_{H0} \cdot x_F\right)}{l_{xy0}}\Delta\psi} - 1\right) \tag{28}$$

Step 3

For small linear and angular displacements, represented by a general variable x, equation (28) converges to:

$$\sqrt{1+x} - 1 \approx \frac{x}{2} \tag{29}$$

which can be numerically and even analytically (exactly) proved, or found in textbooks, once again using L'Hopital's rule.

Hence

$$\Delta l_{xy} = l_{xy0}\left(-\frac{\cos\gamma_{H0}}{l_{xy0}} \cdot \Delta x - \frac{\sin\gamma_{H0}}{l_{xy0}} \cdot \Delta y + -\frac{\left(-\cos\gamma_{H0} \cdot y_F + \sin\gamma_{H0} \cdot x_F\right)}{l_{xy0}}\Delta\psi\right) \tag{30}$$

and finally

$$\boxed{\Delta l_{xy} = -\cos\gamma_{H0} \cdot \underline{\Delta x} - \sin\gamma_{H0} \cdot \underline{\Delta y} + -\left(-\cos\gamma_{H0} \cdot y_F + \sin\gamma_{H0} \cdot x_F\right)\underline{\Delta\psi}} \tag{31}$$

Step 4

Incorporating (31) into (20), and adopting a similar operation as in the previous step, one comes to the following expression

$$\Delta l' \cdot \cos\gamma_V = \frac{l_{xy0} + \Delta l_{xy}}{l_0}\left(1 - \frac{1}{\frac{l_{xy0}}{l_0^2} \cdot \Delta l_{xy} + \underline{\frac{1}{2l_0^2} \cdot \left(\Delta l_{xy}\right)^2} + 1}\right) \tag{32}$$

Step 5

Disregarding the underlined term in (32) as higher order infinitesimal, we have

$$\Delta l' \cdot \cos\gamma_V = \frac{l_{xy0} + \Delta l_{xy}}{l_0}\left(1 - \frac{1}{1 + \frac{l_{xy0}}{l_0^2} \cdot \Delta l_{xy}}\right) = \frac{l_{xy0} + \Delta l_{xy}}{l_0}\left(\frac{\frac{l_{xy0}}{l_0^2} \cdot \Delta l_{xy}}{1 + \frac{l_{xy0}}{l_0^2} \cdot \Delta l_{xy}}\right) \tag{33}$$

Step 6

In (33), the denominator in parenthesis of the last expression can be made equal to unity:

$$\Delta l' \cdot \cos\gamma_V = \frac{l_{xy0} + \Delta l_{xy}}{l_0} \cdot \frac{l_{xy0}}{l_0^2} \cdot \Delta l_{xy} = \\ = \frac{l_{xy0}\left(l_{xy0} \cdot \Delta l_{xy} + \Delta l_{xy0}^2\right)}{l_0^3} \qquad (34)$$

Step 7 (final)

Neglecting the higher order infinitesimal, as in step 5, we finalise with:

$$\Delta l' \cdot \cos\gamma_V = \frac{l_{xy0}^2 \Delta l_{xy}}{l_0^3} = \frac{\Delta l_{xy}}{l_0} \cos^2\gamma_{V0} \qquad (35)$$

Although many steps have been performed so far, they are absolutely justifiable and do not introduce appreciable inaccuracies. This will be evidenced numerically in the last chapter. The listed steps, sometimes repeatedly applied, could have been integrated to some extent, but the adopted approach keeps short-length formulas and ensures clarity.

The horizontal mooring force ultimately reads:

$$F_{xy} = \Delta l_{xy} \cdot \frac{\cos^2\gamma_{V0}}{l_0} \cdot \frac{\mathrm{MBL}}{e_{\%}} \qquad (36)$$

and, after implementing (31):

$$F_{xy} = \begin{bmatrix} -\cos\gamma_{H0} \cdot \underline{\Delta x} - \sin\gamma_{H0} \cdot \underline{\Delta y} + \\ -\left(-\cos\gamma_{H0} \cdot y_F + \sin\gamma_{H0} \cdot x_F\right)\underline{\Delta\psi} \end{bmatrix} \cdot \\ \cdot \frac{\cos^3\gamma_{V0}}{l_{xy0}} \cdot \frac{\mathrm{MBL}}{e_{\%}} \qquad (37)$$

Let's remember that $\Delta\psi$ in (31) is expressed in radians. For small displacements, the vertical angle γ_V converges to its initial value γ_{V0}. The same can be said with regards to the behaviour of the horizontal angle γ_H, which will be explicitly used in the next chapter. In other words, <u>both angles are practically preserved</u>. The horizontal angle has not been focused on in the above transformations, where attention has been paid to the vertical plane of the rope, but an analogy between the two exists.

Static equilibrium for full mooring layout

Let's assume that the static equilibrium of a ship is expressed in its coordinate system. This is natural, since the environmental loads of current, wind, and wave are determined and published in such a system. In view of the definitions introduced in this paper, where both ship- and berth-fixed reference systems initially coincide, this statement is purely formal.

The horizontal restraint force for a single rope, now marked with the '*i*' subscript, is expressed by:

$$F_{xyi} = \Delta x \cdot A_i + \Delta y \cdot B_i + \Delta\psi \cdot C_i \qquad (38)$$

where A_i, B_i, C_i are 'rope-specific' (more precisely – mooring layout-specific) constants, see (37) for details.

This force can be decomposed into the following components:

longitudinal restraint

$$F_{xi} = F_{xyi} \cdot \cos\gamma_{Hi} \approx F_{xyi} \cdot \cos\gamma_{H0i} \qquad (39)$$

transverse restraint

$$F_{yi} = F_{xyi} \cdot \sin\gamma_{Hi} \approx F_{xyi} \cdot \sin\gamma_{H0i} \qquad (40)$$

(yaw) moment restraint

$$M_{zi} = F_{xyi} \cdot \left(x_{Fi} \sin\gamma_{Hi} - y_{Fi} \cos\gamma_{Hi}\right) \approx \\ \approx F_{xyi} \cdot \left(x_{Fi} \sin\gamma_{H0i} - y_{Fi} \cos\gamma_{H0i}\right) \qquad (41)$$

Embedding (38):

$$F_{xi} = \Delta x \cdot A_{fxi} + \Delta y \cdot B_{fxi} + \Delta\psi \cdot C_{fxi} \qquad (42a)$$

$$F_{yi} = \Delta x \cdot A_{fyi} + \Delta y \cdot B_{fyi} + \Delta\psi \cdot C_{fyi} \qquad (42b)$$

$$M_{zi} = \Delta x \cdot A_{mzi} + \Delta y \cdot B_{mzi} + \Delta\psi \cdot C_{mzi} \qquad (42c)$$

where A_x, B_x, C_x, $x \in \{$'*fx*', '*fy*', '*mz*'$\}$, are nine newly defined mooring layout-specific constants.

If the total environmental load to be withstood by *n* number of mooring ropes is depicted by its longitudinal force, F_{Ex}, transverse force, F_{Ey}, and yaw moment, M_{Ez}, then the linear static equilibrium equations take the matrix form:

$$\begin{bmatrix} F_{Ex} \\ F_{Ey} \\ M_{Ez} \end{bmatrix} = -\begin{bmatrix} A_{fx} & B_{fx} & C_{fx} \\ A_{fy} & B_{fy} & C_{fy} \\ A_{mz} & B_{mz} & C_{mz} \end{bmatrix} \cdot \begin{bmatrix} \Delta x \\ \Delta y \\ \Delta\psi \end{bmatrix} \qquad (43)$$

where the global constants (for the whole mooring layout) in the first matrix on the right-hand side of the equation, are summations of particular contributions from each rope, as exemplified by

$$A_{fx} = \sum_n A_{fxi} \ \text{ etc.} \qquad (44)$$

The minus-sign on the right-hand side of (43) comes from the fact that we need to have opposite mooring forces that balance the environmental forces, i.e. the sum of all forces must equal zero.

The equations in (43) shall be solved against the ship's linear and angular displacements as the

unknowns – Δx, Δy, $\Delta\psi$. The set of linear equations is analytically and easily solvable. There are plenty of algorithms in literature and ready computer tools to do so.

For practical assessment or application in navigation practice, the very small radian value obtained for $\Delta\psi$ shall be directly converted to degrees. As stated above, the degree value of heading deviation is also small.

When the displacements from (43) are substituted into (38) we acquire the mooring load in a particular rope. Since in many cases we are mostly interested in the mooring load related to (divided by) MBL, this dimensionless quantity, F'_{xy}, taken as the safety factor, could be directly gained if we omit MBL in computations of equation constants. Therefore, we can base the whole algorithm on the right-hand expression of the below equation:

$$F'_{xy} = \frac{F_{xy}}{\mathrm{MBL}} = \Delta l_{xy} \cdot \frac{\cos^3 \gamma_{V0}}{l_{xy0}} \cdot \frac{1}{e_{\%}} \qquad (45)$$

The dimensionless load F'_{xy} is thus linearly dependent on the ratio of actual dimensionless elongation $\Delta l'_{xy} = \Delta l'_{xy}/l_{xy0}$ in the horizontal plane to the specific elasticity of the rope. However, the environmental force components in the left-hand side of (43) should also be divided by MBL. This approach is thus not practical if different MBLs are present in the mooring layout.

One can also notice that the value of rope elasticity $e_{\%}$, higher for fibre ropes and lower for wire ropes, does not influence the load distribution. The higher the value of elasticity, the higher are the ship's absolute displacements, but the rope force is preserved.

Numerical example and method assessment

Let us consider the practical mooring layout presented in Figure 5. It consists of 8 ropes. The ship's fairleads are marked with small black solid dots. The shore bollards (hooks) are indicated by big white-filled circles. All horizontal geometric properties (with the ship's length of approx. 300 m) can be easily determined. Together with vertical angle data, they are also more accurately summarised in Table 1 in order to document the following numerical calculations. The MBL of 2400 kN and $e_{\%} = 0.02$ are assumed. The former value seems to be large in light of the mentioned ship's size, but it represents the usual navigational practice of doubling ropes sent from the same fairlead. In this way, having nominally 16 ropes (of actual, physical MBL = 1200 kN ≈ 120 t), we can

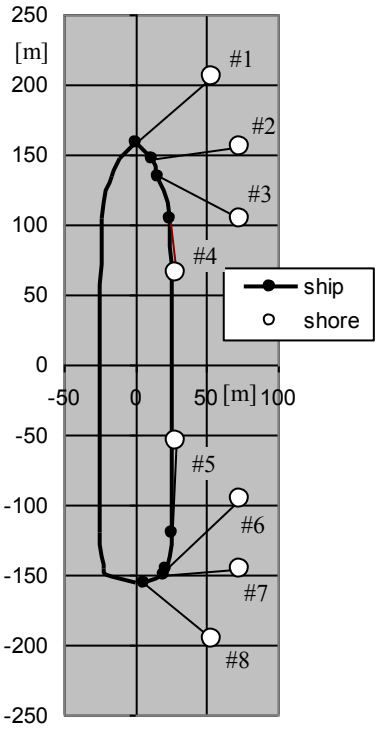

Figure 5. Exemplary mooring layout

essentially restrict our algorithm to 8 different ropes ($n = 8$). The directly obtained load in kN, and its relation to MBL, is relevant to each single rope (total of 16).

Table 1. Input data

Rope ID.	Rope type	x_F [m]	y_F [m]	l_{xy0} [m]	γ_{H0} [°]	γ_{V0} [°]
#1	head line	158.73	0.00	70.82	49.2	12.0
#2	forward breast	147.67	11.04	63.01	83.3	13.5
#3	forward breast	134.07	16.56	64.07	117.0	12.8
#4	forward spring	104.47	23.62	39.82	172.1	20.1
#5	aft spring	–120.47	25.00	65.61	3.6	12.5
#6	aft breast	–145.12	21.47	72.28	46.1	7.5
#7	aft breast	–149.80	19.94	53.87	84.9	10.0
#8	stern line	–155.75	5.83	61.86	129.4	8.8

The input environmental force chosen as an example, corresponding to a 20 m/s wind blowing from behind the beam, is taken as:

F_{Ex} = +114 kN (to forward),
F_{Ey} = –2357 kN (to port),
M_{Ez} = +102 533 kNm (to starboard).

In the case of a fully nonlinear model, numerical computation has been attempted. Having a set of three nonlinear equations with three unknowns, this was essentially an iterative process of manual (trial and error) tuning. Independent and coupled

calibrations of Δx, Δy, and $\Delta\psi$ were utilized to evaluate the equilibrium force and moment with the proper degree of accuracy (±0.5 kN in force, ±0.5 kNm in moment) as fast as possible. In particular, the heading alteration ($\Delta\psi$) is selected in relation with the transverse departure (Δy) off the berth as to preserve a 'positive' elongation both in the forward and aft part of the ship. For this purpose, one could define and automatically calculate intermediate, local transverse displacements at the fore and aft perpendiculars of the ship. The results of numerical solution of the full model are as follows (all digits are significant for the required accuracy):

Δx = +0.0317 m (to forward),
Δy = –0.2878 m (to port),
$\Delta\psi$ = +0.029735º (to starboard).

which lead to mooring loads presented in Table 2. According to mooring practice and recommendations of (OCIMF, 2013), safe working loads in mooring ropes should be below approx. 50% of MBL. These criteria are also met in our example.

Table 2. Distribution of mooring loads for full model

Rope ID.	F_{xy} [kN]	F_{xy}/MBL [%]
#1	219	9.1
#2	372	15.5
#3	365	15.2
#4	138	5.8
#5	7	0.3
#6	405	16.9
#7	783	32.6
#8	575	24.0

The analytical results of the linearized model, derived in the paper, with one more significant digit are quite identical:

Δx = +0.03165 m (to forward),
Δy = –0.28857 m (to port),
$\Delta\psi$ = +0.0298278º (to starboard).

If such are introduced to the full model, we get (in absolute magnitudes) the sum of longitudinal mooring forces lower by 1 kN, transverse mooring forces lower by 6 kN, and mooring moments lower by 335 kNm, as compared to the numerical nonlinear solution. However, the individual load of each rope only differs by as much as 1 kN (and 0.1% MBL).

One can also notice that in this quite real example the heading variation (less than 0.1º) is almost unnoticeable to navigators and terminal operators, maybe due to the assumed low environmental moment.

Conclusions

The analytical and numerical investigations performed in the present work have evidenced the great potential of a feasible linear analytical solution to the problem of mooring load distribution o among particular ropes for a ship at berth.

A small excursion of a ship from the reference position and alignment produces a small elongation, and a small variation of both the horizontal and vertical angles of the mooring rope. The rope elongation itself, however, may not be neglected as it leads to significant forces acting on the mooring ropes, and thus to identical reactions on the ship. The change of the other two quantities (angle-related ones) can safely be disregarded. Hence, we arrive at the very efficient (quick, accurate, and compact) method of analytical linear solution, which can even be implemented in an electronic spreadsheet.

This essentially 3DOF analysis concentrated on the horizontal planar motions (displacements) of a ship is typical for current and wind environmental concerns only. In the case of 6DOF oscillatory ship motions, like in heavy weather/wavy conditions at the site, the presented approach yields somewhat average (steady) loads, which are not the maximum ones. Therefore, future research will be directed towards the dynamic analysis of the mooring loads and the generalization of the algorithm to account for the omitted ship displacements, such as those pertaining to heave, roll, and pitch motions. Further improvements of the algorithm should include the consideration of pretension of moorings and fender effects, usually applied but neglected in the present analysis.

References

1. Artyszuk, J. (2004) Mathematical Model of the Mooring Rope Assisted Ship Manoeuvring. *Zeszyty Naukowe Akademii Morskiej w Szczecinie* 3 (75), Studies of Navigation Faculty. Maritime University of Szczecin.
2. Bronsztejn, I.N. & Siemiendiajev, K.A. (1996) *Mathematics – an Encyclopedic Guide*. 12th Ed. Warsaw: PWN (in Polish).
3. Chernjawski, M. (1980) Mooring of Surface Vessels to Piers. *Marine Technology* 17, 1 (Jan).
4. Natarajan, R. & Ganapathy, C. (1995) Analysis of Moorings of a Berthed Ship. *Marine Structures* 8, 5.
5. OCIMF (2013) *Mooring equipment guidelines (MEG3)*. 3rd Ed. (impression of the original 2008 edition), OCIMF. Livingston: Witherby Seamanship Intl.